Bulletin of Engineering Geology and the Environment (2019) 78:35–53
Published Online: 31st May 2017
DOI 10.1007/s10064-017-1068-6

Development of a 3D structural model of a mine by consolidating different data sources

Morales M.[1]; Panthi K. K.[2]; Botsialas K.[3]. and Holmøy K. H.[4]

[1, 2]Norwegian University of Science and Technology (NTNU), Trondheim, Norway; [3]TITANIA AS Norway; [4]SINTEF Bygg, Trondheim, Norway

Abstract

Joints and faults are inherent part of the rock mass. In the vast majority of mining slopes, discontinuity structures play an important role in slope stability and may trigger a slope failure. The most important step in understanding the slope failure mechanism is to have a reliable model, which shows how all the discontinuity sets are constituted in the rock mass and how they interact with each other. However, building a fracture model is not a straightforward process, since it needs to combine discontinuity information from a variety of sources, such as detailed slope mapping, borehole logging data and remote sensing technologies. Hence, this manuscript attempts to develop a comprehensive structural model of the complete mine area in an open pit, which is the biggest in Norway with respect to its depth and area of coverage. The manuscript demonstrates on how it is possible to consolidate information from different sources in order to identify typical orientation of the detailed fractures that are associated with the main structural lineaments. The process involves analysis of different sources of data in order to correlate this information into useful evidence about the orientation of the fracture systems in terms of dip and dip direction. Further, the mine is divided in different structural domain and a 3D structural model is developed. As an end result, the domains are kinematically tested with respect to different types of failure modes in both overall slope and bench slope scale of the mine for both hanging wall and foot wall. It is highlighted here that the results presented in this manuscript are the part of the research project called "Decisive Parameters for Open Pit Slopes (DePOPS)".

Keywords: Slope stability, rock mechanics, structural model, mining slope, mining geotechnics.

Acknowledgement

The present research is supported by the mining company and the Research Council of Norway (NFR). Authors are grateful to the management of the mining company for allowing us to use data of the mine and research outcome to be published in this journal. Authors are also grateful to other persons such as Balasz Riglar from Ruden AS for the borehole inspection, Javier Macias and Nghia Trinh at SINTEF for developing the structural database of the boreholes, and Giovanni Gigli and Paolo Farina from GeoApp for providing the LiDAR scanning survey. The authors are overwhelmed to NFR and management of the mining company for providing research grant.

1 Introduction

Building a structural model of a mine site is not a straightforward task. It often involves compiling information from many different sources such as: boreholes, field mapping, remote sensing, aerial images, geophysical investigations and so forth. Villaescusa and Brown (1992) stated that a complete two-dimensional description of joint set characteristics is often difficult to establish due to limited size of rock exposures and access problems while field mapping. In the last 10 years, however, the development of remote sensing technologies has been helpful to map areas with difficult or no access, as shown by Riquelme et al (2016). Nowadays LiDAR and digital photogrammetry techniques are extensively recognized and accepted techniques for discontinuity analysis in hard rock environments (Riquelme et al, 2015). The results of the application of photogrammetry into the investigation of rock discontinuities orientation shows that no significant errors are present if the process is done correctly (Lee et al, 2000). On the other hand, the construction of a structural model is mainly based in the definition of the main joint sets and description of their persistence and frequency. Hudson and Priest (1983), Einstein (1983), and Zhang and Einstein (2000) have studied the intensity and frequency of joint persistence in the rock mass and its effect in the rock slope stability. In this field and with the modern widespread imagery of aerial pictures it is not hard to define orientation and spacing of main lineaments of the areas of interest if good rock mass exposure exists. Nevertheless, this does not provide information about dip of the joint sets linked to these major fault planes.

The development of a structural model is the first stage in building a geotechnical model of a mine site. The value of an early geotechnical assessment has been described as the need to establish an appropriate level of geotechnical risk balanced against other key drivers at each stage of the mine planning process (Hanson et al, 2005). In addition, a geotechnical model can be helpful in providing production optimizations in the mine to mill value chain (Bye, 2006). In general, it is considered that the geotechnical structural model is very important step before modelling the classification of the rock mass. Several authors such as Haines (1991), Bye and Bell (2001), Pantelidis (2009), and Hormazábal (2009) have tried to find a suitable way to correlate rock mass classification systems with the stability of a slope.

In this perspective in mind, this article aims to develop a 3D structural model for a mine based on the jointing database from different sources such as field mapping, remote sensing, aerial scanning and acoustical inspection of boreholes. The article first validates on the credibility of jointing measurements of a selected mine area in comparison with the field mapping data. After validation, the mine area is classified in different joint system class following the approach by Willie and Mah (2004). Thereafter, the article attempts to classify the mine in different domains so that a 3D structural model of the whole mine is developed. Finally, the pit slope is geometrically assessed to find out type of potential failures that may be prevailing in each domain for both hanging wall and foot wall. It is highlighted here that this manuscript is a part of a comprehensive research project called “Decisive Parameters for Open Pit Slopes (DePOPS)”. DePOPS is an innovation project funded by the Mining Company (TITANIA AS) and the Research Council of Norway (NFR). The goal of DePOPS is to develop a susceptibility map of the mine, which is easy to depict future stability issues at this open pit mine. The approach and methodologies proposed in this article may also be practically applied in other civil and mining projects.

2 The project case

The open pit mine has been in operation since 1960. In the orebody, about one third of the rock consists of ilmenite. It is located inside the Åna–Sira anorthosite, and it consists mainly of ilmenite-rich norite, which has previously been interpreted as injected in a crystal mush state in a weakness zone of the enclosing anorthosite. This emplacement mechanism has produced a faint orientation in the ore due to the flow of mush (Diot et al, 2001).

The first pass of the walls of the open pit have an initial single bench height of 15 meters, which is doubled in the second pass to have an overall height of 30 meters. Therefore, overall slope angle of the mine is between 45 to 55 degrees along the mine. The open pit has a length of about 2.8 km, while current depth is close to 240 meters (Botsialas and Mass, 2014).

2.1 Geological setup

2.1.1 Regional geology

A large igneous complex, covering about 1200 square kilometers, dominates the geology in the region where the mine is located. The complex consists of anorthositic, noritic and mangeritic intrusions, and jotunitic to charnockitic migmatites. It was formed in late Proterozoic (930 Ma) and is surrounded by Precambrian gneisses (Duchesne, 2003). It is well known for its three large anorthosite massifs: the Egersund-Ogna (EGOG), the Håland-Helleren (HH), and the Åna-Sira (ÅS) massif, last being where the mine is located (Figure 1).

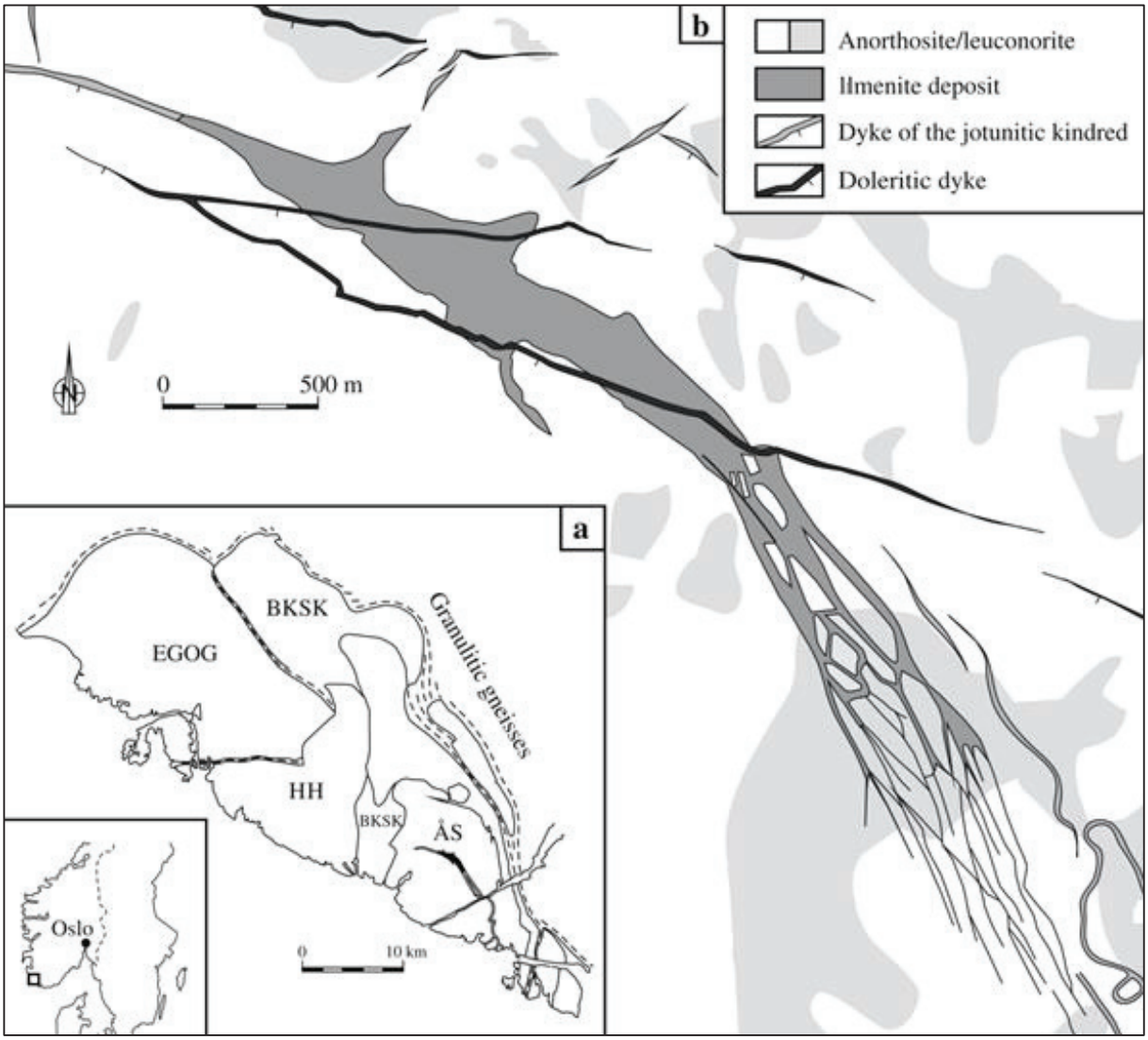

Fig. 1 **a) Geological map of the mine region (modified from Charlier, 2007) presenting the location of the deposit in the central part of the Åna-Sira anorthosite (ÅS). Also showing the anorthosites Håland-Helleren (HH), Egersund-Ogna (EGOG), and the Bjerkreim-Sokndal layered intrusion (BKSK). b) Geological map of the ilmenite deposit (modified from Charlier, 2007).**

The noritic intrusions occurred at a later stage of the genesis, and appeared as several smaller intrusive bodies in the south-eastern part of the province. Some of these norites, like deposit where the mine is located, contain richest ilmenite-bearing deposit known in the world (Marker et al, 2003).

2.1.2 The Åna-Sira massif

The Åna-Sira massif covers more than 100 square kilometres in the region and consists mainly of anorthosite. It is often considered most homogenous of the anorthosites in the igneous complex. The massif hosts significant resources of ilmenite-rich norite where the mine is located. It is described as quite fresh and unaltered anorthosite of medium coarse grain with mega crystalline texture and with grey/violet/brown colouration. The region has been subject to some hydrothermal alteration, which can be seen as white-grey anorthosite, often with shades of pink and green, and with a fine-grained texture. Several small zones of alteration are present (Karlsen, 1997).

The massif is encapsulated by Bjerkreim-Sokndal Lopolith (BKSK) that mainly contains noritic rocks. The anorthosite is cut by several mangerite, noritic and jotunitic dikes, a few bodies of ilmenite norite, a noritic layered intrusion (Bøstølen intrusion) and a swarm of younger diabase dikes. Megacrystic Ca-poor pyroxene appears sporadically. Most common mafic minerals are pyroxene, ilmenite, biotite, amphibole and chlorite (Marker et al, 2003).

2.1.3 Open pit geology

The ilmenite deposit is a world-class Fe-Ti mineralization that consists of an ilmenite rich lens-shaped norite body, which crops out in the central part of the Åna-Sira anorthosite. At both ends it extends into mangeritic dikes, about 5-10 m thick, which stretch to the north-west and to the south-east directions for several kilometres.

The structure of the ore becomes increasingly complex in the east. As shown in Figure 1, xenoliths of anorthosite are present within the ore. The anorthosite, which is located within the ore body or in the contact zones of the ore body, typically shows more alteration than the surrounding rock mass (Karlsen, 1997).

Two major diabase dikes crosscut the ore body in WNW-ESE direction. These have straight appearance and mainly vertical inclination. The largest main dike (furthest to the south) is about 25 meters wide. As main dike exits the ore body in the east, it forms swarm of several smaller dikes extending from the main body. Two distinct faults, the Hommedal and the Tellnesvatn faults, and several smaller fracture systems cut the ilmenite ore body. Several studies have shown that there are some areas of heavy alteration that is related to fractures and fault systems at the mine site, on both ore body and anorthosite.

2.2 Regional structural environment

Karlsen (1997) have categorized seven different regional lineaments present in the mine district. These main lineaments have been identified in the aerial photos and are mapped in GIS to provide a clear understanding of the regional situation as below so that they can be linked to the fracture systems (FS) in the overall pit areas (Figure 2).

- Hommedal (FS1) (N-S)
- Jossingfjord (FS2) (NE-SW)
- Åna-Sira (FS3) (ENE-WSW)
- WNW-ESE (FS4)
- Tellnesmyra (FS5) (NW-SE)
- Crusher (FS6) (NNW-SSE)

Figure 2 shows that there are lineaments, which are associated with local fracture systems may define geometries needed for planar, wedge or toppling failures in condition that the orientation of the pit slope and orientation and characteristic of fracture systems favours.

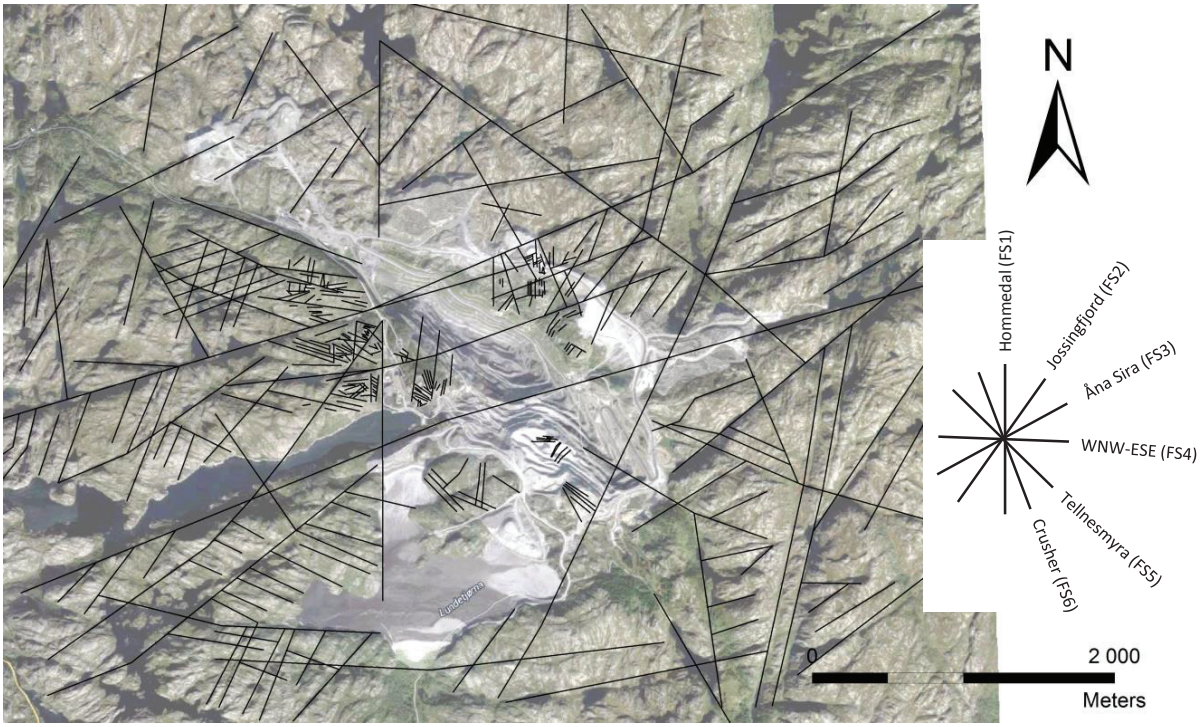

Fig. 2 Illustration of the main lineaments in the mine district. (DEM image source: Norge i bilder)

An assessment of the 2-dimensional lineament traces (Figure 2) gives us information about their approximate orientation as;

- Hommedal lineament (FS1) is oriented close to north-south direction and influences areas in both hanging and foot walls with smaller spaced traces.
- Jossingfjord lineament (FS2) is oriented in northeast-southwest direction and has high density occurrence in the NW and the central-north (footwall) areas of the mine.
- Åna Sira lineament (FS3) presents itself with very long and persistent faults all along the area and is oriented at ENE-WSW.
- WNW-ESE lineament (FS4) has an orientation very close to east-west and is closely spaced fracture system and is very close to parallel to the slope face of the hanging wall in the central portion of the pit.
- Finally, it is not easy to distinguish between Tellnesmyra and Crusher lineaments (FS5 and FS6), as both have variable directions with a strike ranging from N120E to N165E. These lineaments are in some cases overlapping. These two lineaments have greatest influence along the hanging wall as they run also almost parallel to the slope and have similar orientation as of mine axis that runs in NW-SE direction.

3 Validation of the jointing measurements

In order to validate all sources of information from where joints have been acquired, a brief comparison of the jointing in a specified area of the mine (red rectangle in Figure 3) has been carried out. Emphasis has been given for the area where detailed study was carried out in the past; such as study by Nilsen and Ballou (2006) and Botsialas and Mass (2014); and the area where comprehensive field mapping has been carried out under this study. In addition, the selected area also features all sources of information consisting remote sensing, acoustic borehole scanning, LiDAR data and three different field mapping resources (Rock mass classification including joint measurements, geotechnical cells for measuring joint orientation in a certain exposed slope face, and tunnel mapping).

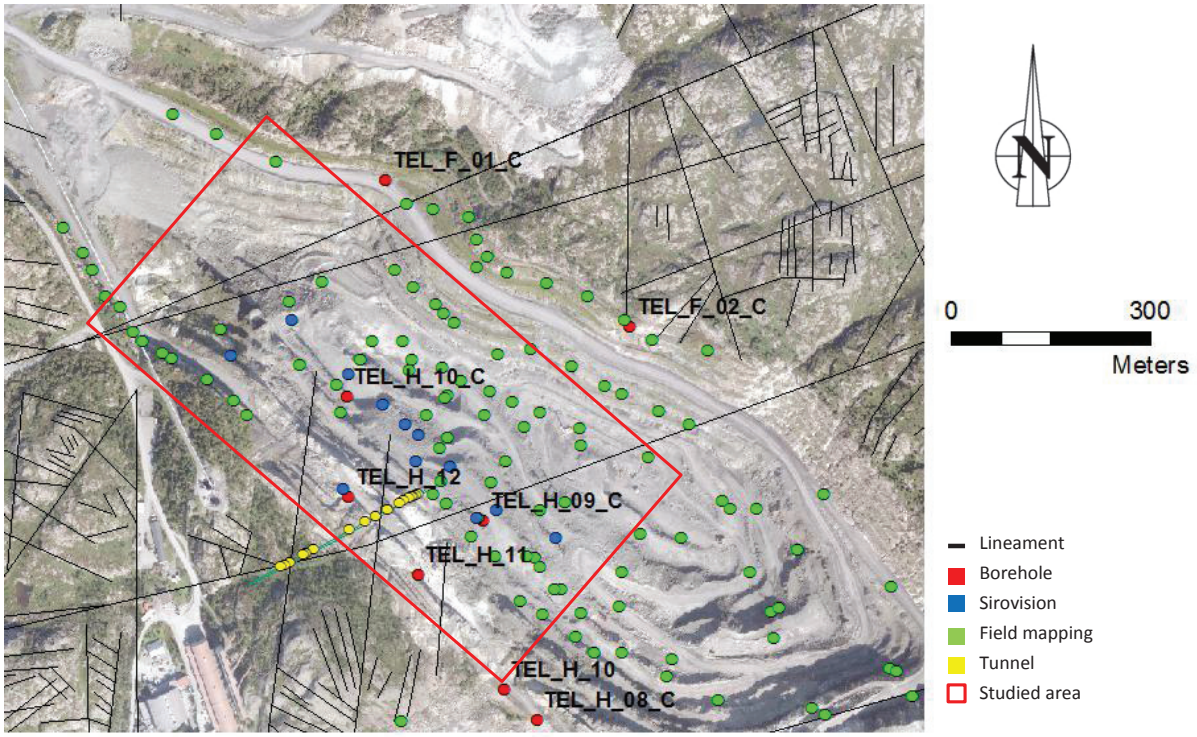

Fig. 3 **Area of study for the structural model. It is clear to see that there are 4 major joint sets present in the area, with orientation N-S, WNW-ESE, NW-SE, and ENE-WSW.**

The area of study itself (red rectangle in Figure 3) contains specific information about detailed jointing condition, in terms of dip and dip direction. The area is almost enclosed between two large lineaments that stretch in the WSW-ENE direction. In addition, the area is limited to the hanging wall of the mine, which is facing NE.

Figure 3 also shows the spatial distribution of four sources of information. As it is possible to see inside the rectangle, the boreholes (in red) considered are named as TEL_H_09_C, TEL_H_10_C, TEL_H_12, and TEL_H_11. The first two boreholes represent core-drilled holes and the other two hammer-drilled holes. There are also twelve 3D images in the selected area (in blue) and field mapping of joint orientations in both slope face (in green) and inside the tunnel located in the area (in yellow). LiDAR measurements have not been indicated in the figure since the number of joints considered is around 800, with more or less homogenous distribution.

3.1 Classification and validation of joint systems

The main objective of this part of analysis is to check a proof of the reliability when combining data from different sources in order to develop a structural model for the pit shown in Figure 3. The following procedure represents a test of the techniques, and it is not intended to provide a detailed analysis of the joint condition, but rather focused in classifying the jointing systems based on the joint orientation.

Four main sources of jointing data available to analyse were employed:

- Remote sensing using photogrammetry supplied by Sirovision (software available at sirovision.dataminesoftware.com).
- LiDAR scanning of the pit. (Gigli and Farina, 2016)
- Field mapping of different benches along the slope face
- Drainage tunnels mapping (Langåker et al, 2015)
- Orientation mapping of discontinuities obtained from acoustical televiewing log of four boreholes mentioned earlier (Riglar and Varga, 2014)

A total of twelve 3D images were analysed using Sirovision software to provide information about jointing orientation. The results obtained were information about dip and dip direction of joints. Data were obtained by tracing contours of fractures that can be identified in 3D images. It is noted here that Sirovision calculates orientation of a plane defined by a trace by solving 3D equations that incorporates points on the trace for parameters of the plane that best fits the trace. Closer a trace is to a straight line more "ambiguous" is the definition of that plane (an infinite number of planes can pass through a straight line) and greater the variation one can observe in the angle of that plane fitted to the trace. This means, more clearly defined or less unambiguous a plane is, more accurate will be the estimate of orientation of the plane. Therefore, following methodology was used for the analysis of the information:

1. Geo-reference each of the positions for analysed 3D images. This was done by locating coordinates of the centre of the reference image.
2. Generate a zone of 100 meters (based on average maximum spacing of previously identified joint systems) around each one of these positions in order to have information about which boreholes and/or field mapping data was in the neighbourhood of the 3D image in consideration.
3. Analyse, via pole-, rosette- and density plots, each of the 12 sets of information: Each sets contains at least two of the following: remote sensing, LiDAR, field mapping (surface and tunnel) and acoustical televiewing of boreholes. All joint sets present in each data source were identified separately, and later on checked in how they correlate with others found in other data sources.
4. Combine all data in each of the 12 sets in order to have a unique rosette and pole diagram for each zone. Then distinguish sets discussed in numeral 3 using the joint sets identified in the 3D images, from field mapping, LiDAR scanning, and from four boreholes present in the area.
5. Finally analyse resulting pole, rosette and density plots and then define distinctive joint sets.

The analysis of rosette, contour and pole density plots was done in Dips (available at www.rocscience.com). The number of available data (in terms of identified joints with its respective measurement of dip and dip direction) was 1059 points in Sirovision, 810 points from borehole imaging, 825 from LiDAR scanning, and 81 from field measurements (49 from geotechnical windows on the slope face and 32 joints identified during tunnel inspection). Figure 4 shows resulting joint rosette plots from all four sources of information. Average dip and dip direction of each of the joint sets were recorded. These findings will be explained in detail in chapter 5.

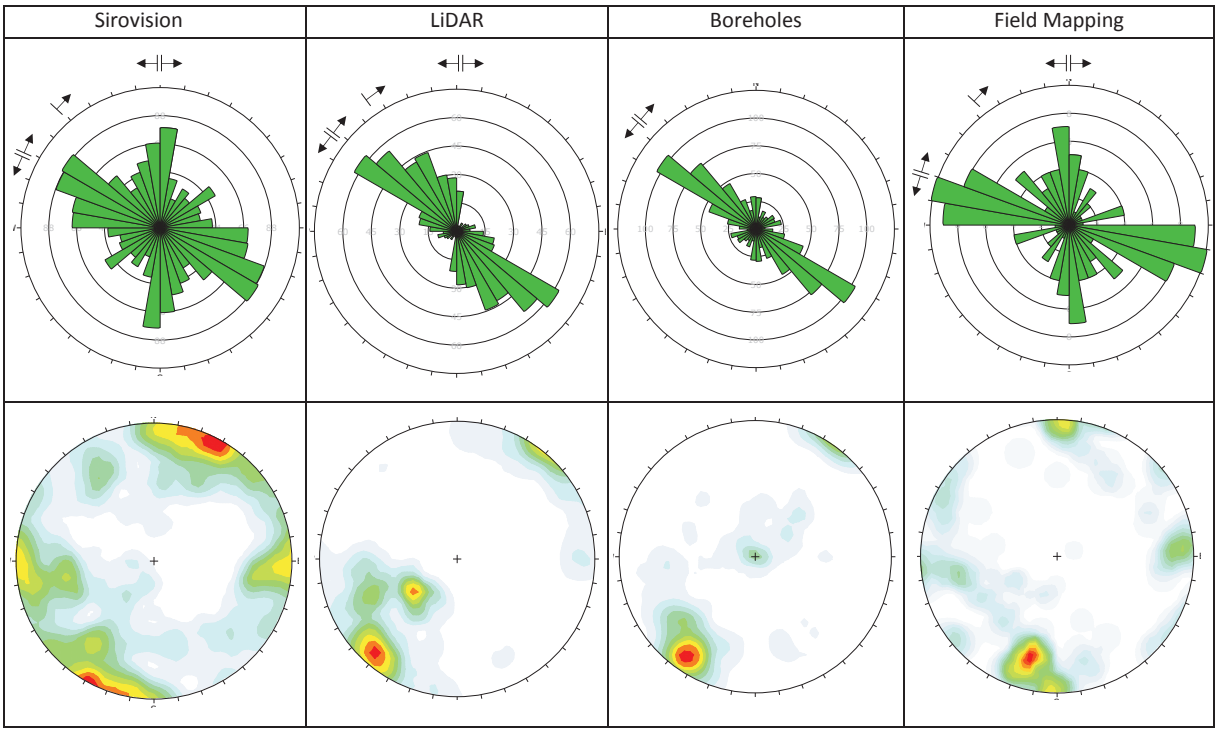

Fig. 4 **Rosette and pole plots for the discontinuities identified in the 3D image remote sensing in Sirovision (left), LiDAR (centre left), borehole information from acoustical televiewer (centre right), and field mapping of the slope face and tunnels (right) in the interest area.**

As can be seen in Figure 4, rosette and pole plots from three data sources excluding data from borehole clearly indicates that the mine is influenced by three distinctive joint systems. In this sense, as the boreholes are orientated near the vertical axis and a blind spot may have been found while sampling fractures that occur nearly parallel to the direction of drilling. Similar conditions were also observed by Park (2002) who described that the number of discontinuities from a given set may be intersected by a sampling line that makes a certain acute angle to the set normal and on the other hand may reduce it to zero when the acute angle approaches 90. Detailed jointing of the mine is interlinked with most of the major lineaments shown in Figure 2 and described by Karlsen (1997). Based on this finding and extent and intensity of occurrence of different joint systems, all joint systems in the mine are further classified in four groups.

- The first joint set (J1), the most prominent one, is running with orientation WNW-ESE and is well correlated with WNW-ESE (FS4) lineament. The field observation indicated that this joint system has spacing ranging from 10 to 20 meters.
- The second joint set (J2) is running in NW-SE direction and is related to the Tellnesmyra (FS5) and the Crusher systems (FS6). The field observation indicated that this joint system has slightly larger spacing than J1 with a typical spacing range from 25 to 50 meters. This set is important in terms of influence on stability of the area, since events of sliding planes have been recorded in the past.
- The third joint set (J3) is running in the N-S direction and is related to the Hommedal fracture system (FS1). This joint set is widely spaced with a typical spacing ranging between 80-120 meters. It is important to note that this joint always intersects both J1 and J2, and is systematically distributed in the studied area.
- The last joint set (J4) is running in the ENE-SW direction and is not very distinctive in Figure 4, which may be related to the Åna-Sira (FS3) fracture system. In the field this joint set is mainly identified close to the north and south boundary of the pit. It is noted here that this joint set has very wide spacing (between 400-500 meters) and hence, there are not many joints parallel with the main lineaments in the considered area.

Further, the joint set (J3) with N-S direction linked with Hommedal fracture system (FS1) has somewhat less density in the rosette and pole plot from LiDAR data. One reason for this might be a bias in the information from LiDAR scanning caused by the direction of scanning device. For boreholes on the other hand, there is only one recognizable joint set (J2) that shows trend in the NW-SE direction and represents the Tellnesmyra (FS5) and the Crusher systems lineaments (FS6). As expected, field mapping data identifies three main joint sets and all of them very well correlate with the ones found in Sirovision plot. J1 that goes in direction WNW-ESE (FS4), J2 in direction NW-SE (FS5 and FS6), and J3 following the N-S trend (FS1). It is however noted here that joint set J2 was not possible to frequently map in the field due to limited access caused by the advance in mining sequence and presence of J2 more to the upper benches of the mine, where access is limited.

Finally, by looking in detail (and with the previous knowledge of the main lineaments) it is also possible to identify some discontinuities aligned in the NE-SW direction both in the Sirovision and in the field mapping data. This joint set could be interpreted as J4, but the amount of data has not been considered enough to conclude that this represents a cluster of discontinuities relevant to the pit slope of the selected area. As the boreholes are orientated in the NE-SW direction and the slope face is NW-SE, NE-SW structures (i.e. the Åna-Sira formations) are uncommon in occurrence.

3.2 Analysis of joint systems information

Taking into account the joint sets classified in previous sub-section and direction of the main lineaments described in sub-section 2.2, all identified joint sets were found to be related and have a consistent correlation with the regional trends of lineaments shown in Figure 2. With this findings, summary of the statistical variating of all fracture systems are presented in Table 1.

Table 1 Statistical distribution of Dip/Strike for the main joint sets found in the studied area of the open pit mine. Angles are in degrees.

Joint set	Sirovision		LiDAR		Boreholes		Field Mapping	
	Dip (direction)	Strike	Dip (direction)	Strike	Dip (direction)	Strike	Dip (direction)	Strike
J1 avg	85 (NE/SW)	N109E	84(NE/SW)	N127E	78 (NE/SW)	N129E	80 (NE/SW)	N101E
Max	*90*	*137*	*89*	*141*	*90*	*154*	*90*	*115*
Min	*78*	*84*	*75*	*121*	*59*	*107*	*65*	*88*
Stdv	*3*	*14*	*4*	*6*	*8*	*11*	*8*	*8*
J2 avg	46 (NE)	N133E	44(NE)	N140E	-	-	56 (NE)	N147E
Max	*57*	*153*	*53*	*162*	-	-	*70*	*170*
Min	*34*	*118*	*33*	*121*	-	-	*32*	*119*
Stdv	*6*	*10*	*6*	*11*	-	-	*13*	*17*
J3 avg	78 (E/W)	N177E	67(NNE)	N174E	-	-	80 (E/W)	N178E
Max	*90*	*191*	*77*	*168*	-	-	*88*	*197*
Min	*60*	*161*	*58*	*152*	-	-	*70*	*78*
Stdv	*9*	*8*	*5*	*4*	-	-	*5*	*10*
Total joints	1059		469		810		81	

As shown in Table 1, the first joint set (J1) has an overall average strike/dip of N113E/81. In terms of dip direction it is possible to find joints in both ways (i.e. close to 023 and 203 degrees) and it is very well correlated with the WNW-ESE fracture system (FS4). As has been identified before, this joint set is the one with the closest spacing, and thus is considered the most important in terms of influence in bench scale stability. This joint set also represents the most dominant joint set identified through the analysis of boreholes data as shown in Figure 4.

The second joint set (J2) has a global strike/dip of N140E/48NE and, again, a good correlation with the Tellnesmyra (FS5) and Crusher (FS6) lineaments. This joint set is comparable with the description of an unfavourable joint system

(Crusher system, FS6) in the hanging wall as described by Nilsen and Ballou (2006), who stated that typical strike of these joints is N115- 160E, and the dip is typically 40-50 degreed to NE. In addition, Botsialas and Mass (2014) describe a set of fractures with an approximate strike/dip of N145E/45NE that belongs to the Crusher fracture system. This system is oriented oblique to the longest axis of the pit. It is clear that the crusher system (FS6) lineament is the one that is more related to this joint set, but in some cases, there could be an overlap between FS5 and FS6 that may lead to an intermediate joint set that dips in angles higher than 60 degrees. This intermediate joint set may be the product of interaction between these two structural systems. As FS5 and FS6 are constantly overlapping in terms of strike/dip, it is worthwhile to point out that the dip angle associated to the Tellnesmyra lineament (FS5) are usually having a dip angle close to 75 degrees, while for the Crusher system (FS6) the dip angle is falter with the range of 40-50 degrees.

The third joint set (J3) has a general strike/dip of N176E/75W, but here again, it is possible to find joints with a dip direction in both ways (i.e. close to 266 and 86 degrees). This third system of joint set is aligned in the same direction as the Hommedal (FS1) fracture system.

Evidence of distinctive discontinuities in the direction of Åna-Sira lineament have not been found as a joint set of importance in the study area, however as described in the previous sections, there are some structures aligned in this direction, which are described as J4. It seems that there is no considerable influence of the trends of this system in the jointing of the pit, because they do not generate an associated joint system in the space between two mapped lines. Hence, this lineament does not influence other discontinuities in the rock mass but rather creating local zones of weakness around the faults.

3.3 Discussions on the correlation

Four different approaches in discontinuity mapping presented above gave good confidence level in defining representative orientation of the joint systems. The main benefits of these techniques are that there are increased possibilities of assessing for example; a) areas that are not accessible by using Sirovision and LiDAR, b) the evaluation of jointing direction behind the exposed slope by using borehole acoustical televiewing and c) the reliability testing through direct field measurement using engineering geological field mapping. The analysis also demonstrated that there is a good correlation between joint sets found with the main lineaments mapped with the help of aerial photos. The analysis also gave possibility to identify both orientation and dip of the most important and influencing fracture systems of the open pit.

The deviation founds from other three methods in relation with field mapping are considered to be within the acceptable limit. Associated deviation of Sirovision measurements is with an average of 6.3% in dip and 4.3% in strike. Similarly, for LiDAR mapping, the deviation is with an average of 9.6% in dip and 7,6% in strike. Finally, for the borehole, the deviation is with an average of 2.2% in dip and 15.6% in strike. One important information achieved with this analysis is that, if carefully done, the detailed jointing information may equally be trustworthy form both Sirovision and LiDAR techniques. However, borehole data may not give detailed information of the different joint sets due to not being able to hit all the joint systems in a confined area of borehole location. Hence, both Sirovision and LiDAR techniques are found to especially useful for mapping remote areas with difficult access. Another finding of this analysis is that WNW-ESE fracture system (FS4) is correlated with joint set (J1) and has an overall average Strike/Dip of N113E/81. The Crusher lineament (FS6) is related to joint set (J2), with an average orientation of N140E/48. Finally, the Hommedal fracture system (FS1) is associated to the third joint set (J3), and has an average orientation of N178E/79. An interpretation of the Åna Sira (FS3) could be understood as joint set (J4) with an average orientation of N125E/79, which is seen in the pole plots of Sirovision and field mapping data with relatively less density.

4 Definition of structural domains

The jointing data analysed are distributed in different depths of the pit slope. In this perspective, it is worthwhile to perform an analysis dividing the slope based on what is possible to observe in the field. From bench 145 masl and upwards, the joint set (J2) linked with the Crusher system (FS6) is mainly influencing on the pit slope stability. On the other hand, in the lower benches (below 145 masl) this joint system is not as pronounced as in the upper benches

above 145 masl. Therefore, other joint sets such as joint sets (J2) related to Tellnesmyra (FS5), joint set (J3) related to Hommedal (FS1) and joint set (J1) related to WNW-ESE (FS4) are more relevant. Hence, the joint information was split in two datasets, with bench at elevation 145 masl as defining this limit. The resulting pole plots are shown in Figure 5.

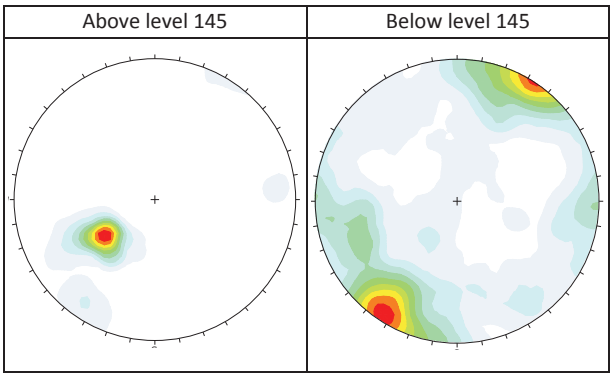

Fig. 5 Pole plots for the discontinuities above and below level 145 masl.

As can be seen in Figure 5, the joint set (J2) related to Crusher system (FS6) is the only prevailing set dominating above bench level 145 masl. Faint evidence of J2 related to Tellnesmyra (FS5) and J3 related to WMW-ESE (FS4) are also found. On the other hand, below level 145 masl it is possible to identify 3 joint sets such as J2 related to Tellnesmyra (FS5), J3 related to Hommedal (FS1) and J1 related to WNW-ESE (FS4). Hence, in the following, joint set data for the whole pit is analysed by dividing the pit above 145 masl and below 145 masl.

4.1 Analysis of joint information

For the definition of structural domains, database containing all joints from different sources were first collected. The total data set consisted are of 16161 joints from different mapping sources as indicated in Table 2.

Table 2 Distribution of joint data by source.

Source	Number of joints
Sirovision	5.793
LiDAR	2.815
Boreholes	3.757
Field Mapping	3.796
Total joints	16.161

A script in Visual Basic (VBA) was developed for further analysis of the database by selecting joints contained inside certain volume, where volumes were defined as cubes. The idea behind the script was to select size of the cube in which joint orientation is analysed as a sort of resolution of the detailed jointing in each zone of the mine. The goal is to define a three-dimensional distribution of joint sets based in the cubes. Gigli (2014) has shown that it is possible to obtain average orientation of a given joint set based in this way of analysis of different observations confined within a given volume.

A detailed study of the data showed that maximum persistence measured for the major lineament in the pit area is 240m long and an average of the most persisting 20 lineaments is found to be 142m long. On the other hand, average detailed jointing persistence in the pit area is 12m long. Therefore, it is decided that the resolution should be a value closer to the maximum joint persistence in order to try to keep long discontinuities confined in no more than 3 different cubes. Considering this in mind, a block size of 200m was found to be an optimum size for the cube. In order to fix upper and lower limits of the cube, maximum and minimum elevations were fixed at 343 masl and -50 masl,

respectively. Since total elevation coverage is close to 400, it is decided to limit the cubes in two elevation levels; i.e. cubes above elevation 145 masl and below this elevation level, which is also in line with the intermediate bench level. Subsequently, the lower cubes represent cubes between elevation levels -55 masl and 145 masl. Similarly, upper cubes represent cubes between elevation level of 145 masl and 345 masl. With this division, 8391 joint database will represent below elevation of 145 masl and 7770 joint database above this elevation, respectively.

Further, to have a better idea on the quantity of measurements inside each cube, count of the joints was done in ArcMap for both upper and lower elevation database. The purpose here is to have a basic index of "reliability" defined by the number of measurements (or joints) inside each cube. The reliability index is needed to safeguard representativeness of the sample. The sample size (number of joints in a cube) is calculated using Equation 1 proposed by Yamane (1967).

$$n = \frac{N}{1+Ne^2} \quad (1)$$

where, n : sample size
N : size of the population
e : level of precision

Five levels of precision are found to be representative reliability class consisting 1%, 5%, 10%, 15%, 20%, and 30%. 1% is defined as very high reliability, 5% is defined as high reliability, 10% as normal reliability, 15% as low reliability, 20% as very low reliability, and 30% as non-reliable. The concept of precision is related to the sampling error and is the range in which true value of the population is estimated to be. Reliability index of the jointing database for both upper and lower elevation of 145 masl defined based on Equation 1 is presented in Table 3.

Table 3 Division of joint dataset in reliability classes for lower and upper elevation from 145 masl.

Reliability class	-55to +145 Population (N) = 8391		+145 to +345 Population (N) = 7770	
	e	n	e	n
Very high	1 %	4563	1 %	4373
High	5 %	382	5 %	380
Normal	10 %	99	10 %	99
Low	15 %	44	15 %	44
Very low	20 %	25	20 %	25
Non-reliable	30 %	11	30 %	11

As indicated in Table 3, zero to 10 joints contained inside the cube is classified as non-reliable, and treated as unreliable for further analysis. From 11 to 25 measurements contained inside the cube are considered as reliability class very low and from 26 to 45 as low. From 46 up to 100 datasets confined within the cube is considered as reliable and datasets confined above 380 are considered very high reliable.

This reliability class is then used as basis to develop jointing zonation system in ArcMap (Figure 6). As can be seen in the figure, most of the cubes outside the mine area have less than 10 measured dataset of joints for both upper and lower elevation of 145 masl (squares in red) with exception for the mine area where very limited mapped database were available due to limited accessibility and shadow effect. Normal and high reliability zones (in green) exceeding 99 dataset of joints for lower bench levels (below 145 masl) are highly concentrated along the central part of the mine where lower benches are exposed. On the other hand, upper levels (above 145 masl) with high and normal levels of reliability (in green) are concentrated in the upper benches (i.e. close to the pit limits).

Finally, datasets of the joints from respective cubes were exported to Dips to plot rosette diagrams and these were introduced into ArcMap as shown in Figure 6.

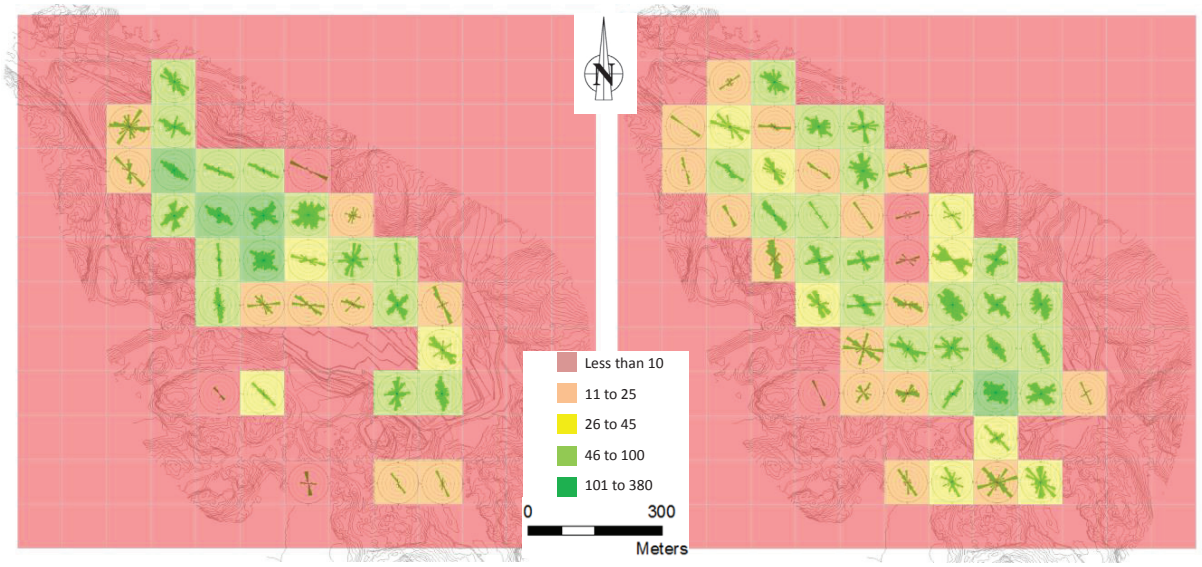

Fig. 6 **Count of joint information and rosette diagram per cube for the bottom level (elevation -55 to +145, left) and upper (elevation +145 to +345, right).**

4.2 Structural zonation of the pit

The geotechnical zonation of the mine was done taking into account rosette plots obtained for each cubical quadrant in both lower and upper elevation level of 145 masl. A total of 7 structural domains were identified in the lower portion of the mine, while 8 were identified for the upper levels from 145 masl. Each structural domain was defined analysing both rosette and pole plots (Figure 6). For each structural domain a polygon was traced and rosettes and pole plots were developed for each of them (Figure 7 and Figure 8).

4.2.1 Elevation level -55 and +145

The first structural domain is named SD145_01, which represents structural domain at elevation level of 145 masl (the elevation of the overall cube). This structural domain shows clear dominance of joint systems that are oriented in NW-SE direction and have an average dip/dipdir of 90/029. This joint set represents approximately 20% of total joints observed in this structural domain. There is a second joint system with less dominance that has an orientation of N-S direction with dip/dipdir at 89/269. As seen in Figure 2 and Figure 7, both these joint sets have orientation similar to Tellnesmyra (FS5) and Hommedal (FS1).

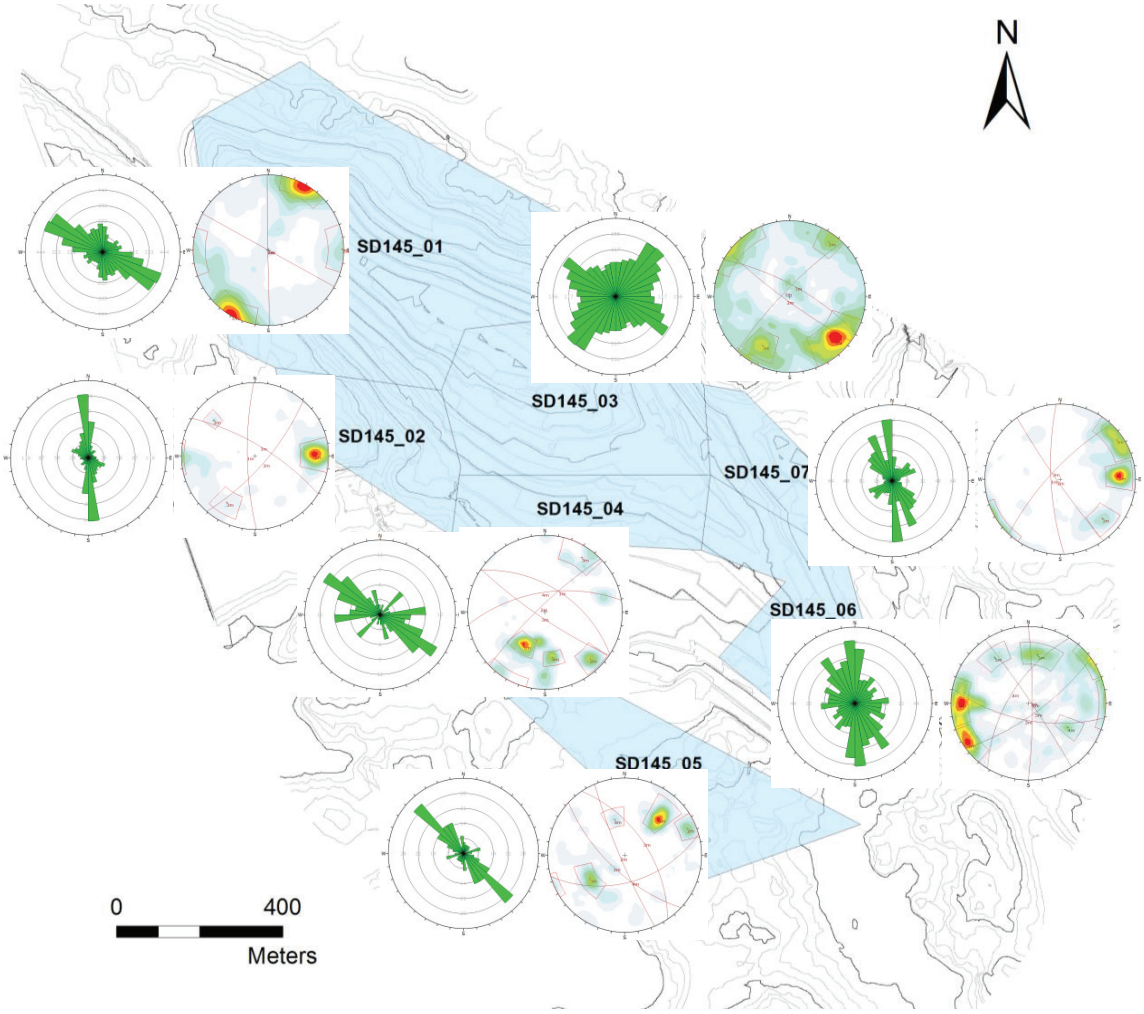

Fig. 7 **Rosette and pole diagrams per structural domain for the bottom level (elevation -55 to +145)**

The second structural domain named SD145_02 (Figure 7) shows only one very distinctive joint set in N-S direction at 78/269. As can be seen, this joint system has very close to same strike direction as of the second joint set identified in SD145_01, but slightly lower dip angle. This structural domain has a density of 27% of the observations, and orientation coincides with the Hommedal (FS1) lineament as indicated in Figure 2.

The third structural domain named SD145_03 (Figure 7) on the other hand shows two major joint system orientations. The first one is in NE-SW direction, close to the orientation of the Jossingfjord (FS2) lineament as described in Figure 2. This joint system has an orientation (dip/dipdir) of 80/314 and represents 20% density of the observations. The second joint system has an orientation of NW-SE direction, again in line with the Tellnesmyra (FS5) lineament. The average dip/dipdir of this joint system is 73/029.

The fourth structural domain maned SD145_04 has two distinctive joint systems. The first one runs in NW-SE direction and has dip/dipdir of 54/033. This joint system resembles with the Crusher system (FS6) and has density of 21% of the observations. The second joint system runs in E-W direction, which resembles with WNW-ESE (FS4) lineament. This joint system represents 12% of the observations and has dip/dipdir of 81/214. One can also identify two minor joint sets in this structural domain having dip/dipdir of 80/316 and resembling the Jossingfjord (FS2) lineament and another joint system has dip/dipdir of 61/351 representing the Åna Syra (FS3) lineament.

The fifth structural domain named SD145_05 shows clear evidence of only one dominant joint system that has an orientation of NW-SE direction. Analysing the pole plot gave us additional information about the trend, which

indicates both Crusher (FS6) and Tellnesmyra (FS5) system with dip/dipdir angles of 57/052 and 66/223, respectively, and represents 19% and 14% of the observations.

The sixth structural domain named SD145_06 shows three system of joints, which resembles with Hommedal (FS1), Tellnesmyra (FS5), and WNW-ESE (FS4) lineaments. The orientations of these joint systems are 86/056, 84/090 and 64/191, respectively and have 10%, 13% and 11% density of the observations, respectively.

The seventh structural domain named SD145_07 shows evidence of two systems in N-S and NW-SE direction that represent Hommedal (FS1) and Tellnesmyra (FS5) lineaments. The orientation of these joint systems are 76/267 and 85/235 and represent 16% and 18% of the total observations.

4.2.2 Elevation level above +145

Eight structural domains were identified in the benches above elevation 145 masl (upper benches) following same structural domain indicated in the previous section (Figure 8).

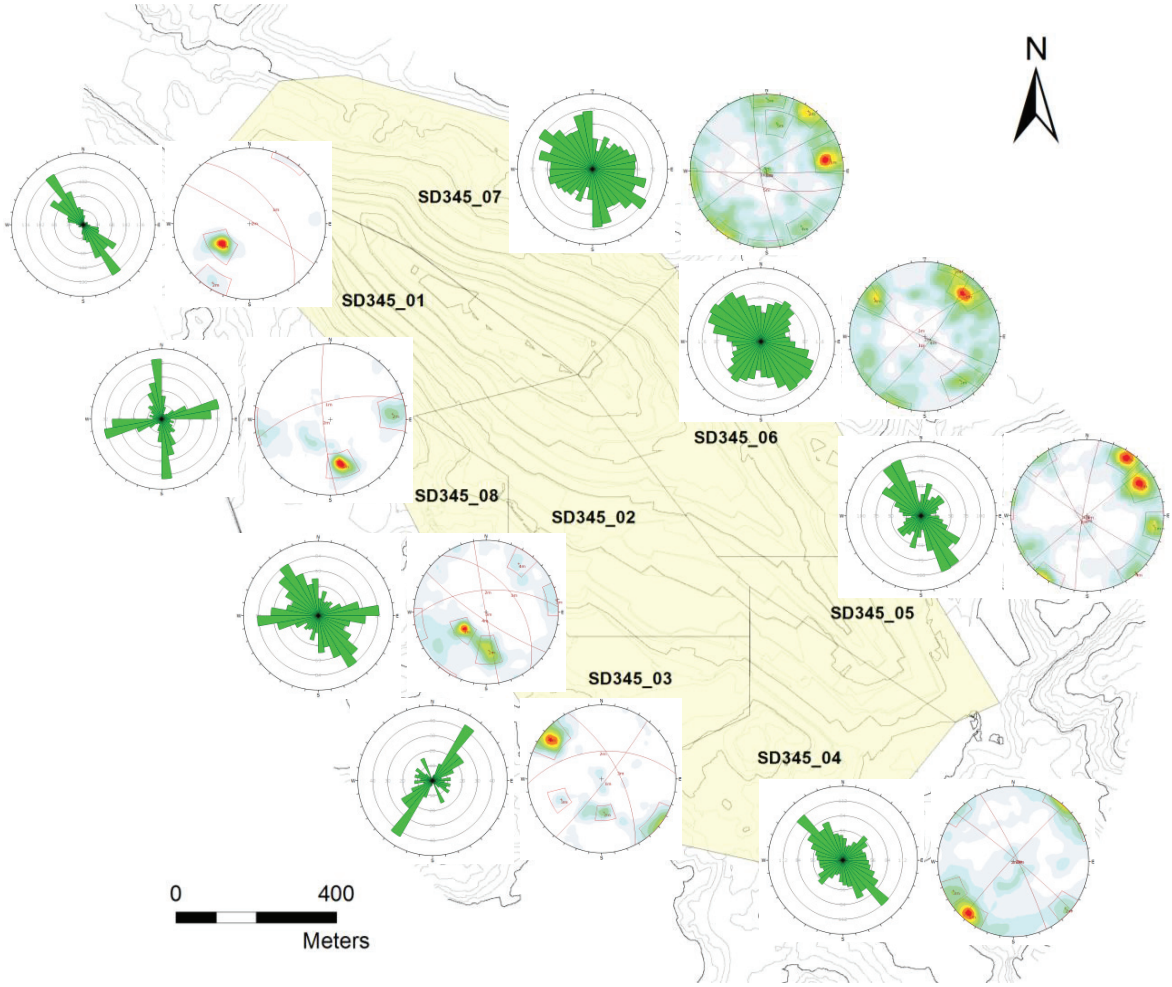

Fig. 8 Rosette and pole diagrams per structural domain for the upper level (elevation +145 to +345)

The first structural domain named SD345_01 shows a clear dominance of structures aligned in NW-SE direction, with an average dip/dipdir of 49/054 and represents 50% of the total joints observed. This joint system is in close proximity with the Crusher system (FS6). It is also possible to note a second slightly less density (9% of observed) joint system oriented in NNW-SSE direction with dip/dipdir of 85/032, which is in close proximity with the Tellnesmyra (FS5) lineament.

The structural domain named SD345_02 shows two distinctive jointing systems oriented in NW-SE and E-W directions. The first one has a dip/dipdir of 43/052, and it is interpreted as part of the Crusher system (FS6) due to its low dipping angle and represents 16% density of the observations. The second joint system has dip/dipdir of 56/356 and has almost similar density as the first one. This joint system resembles with direction of the WNW-ESE (FS4) lineament, but dip angle is not as steep as the previous observations.

The third structural domain named SD345_03 shows only one major orientation in the NE-SW direction similar as direction of the Jossingfjord (FS2) lineament. It has a dip/dipdir of 84/128 and represents 27% density of the observations.

The fourth structural domain named SD345_04 has also one distinctive joint sets running in NW-SE direction with dip/dipdir of 85/040 and this joint system is associated with Tellnesmyra system (FS5) and has 11% density of the observations. As Figure indicates, several less important (in terms of percentage) joint sets could be interpreted in this area, with a large number of joint sets that are orientated in diverse directions.

The fifth structural domain named SD345_05 shows clear evidence of two dominant joint systems that run NW-SE direction. These joint systems represent both Tellnesmyra (FS5) and Crusher systems (FS6). These joint systems have dip/dipdir angles of 78/239 and 85/213 and represents 15% and 11% of the observations, respectively. There are also two low density joint systems associated to Jossingfjord (FS2) and Åna Sira (FS3) lineaments, with dip/dipdir of 83/279 and 89/320, respectively. These two joint systems represent approximately 6% volume each.

The sixth structural domain named SD345_06 shows high degree of dispersion, but it is still possible to find directions that correlate with Åna Sira (FS3), Tellnesmyra (FS5), and WNW-ESE (FS4) lineaments. Their orientations are 74/321, 76/224 and 80/127 and represent density distribution of 7%, 9% and 6%, respectively.

The seventh structural domain named SD345_07 shows evidence of three systems in N-S, E-W, and NW-SE direction, correlated with Hommedal (FS1), Tellnesmyra (FS5), and WNW-ESE (FS4) lineaments, with orientations of 80/260, 87/215, and 87/180, respectively. These joint systems represent joint density of 11%, 6%, and 5% of the observations, respectively. One can also find some evidence of the Åna Sira (FS3) lineament having orientation of 81/328.

Finally, the eighth structural domain named SD345_08 shows two very distinctive joint systems in N-S direction with dip/dipdir of 79/265 and in WSW-ENE direction with dip/dipdir of 63/345. The first set represents 27% of the total observations, and its orientation coincides with the Hommedal (FS1) lineament. The second joint has 12% of the total records, and it is aligned in the direction of WNW-ESE (FS4) lineament.

5 3D structural model

Following these structural domains developed in section 4, contours of each domain were traced in ArcGIS and then exported this information into Leapfrog to develop a 3D structural model. The basic concept with this development is to create volumes that resemble contours of the domains obtained by analysing joints inside the cubes that cover whole area of mine.

For both below and above 145 masl elevation levels contours were placed in the mid elevation, i.e. +45 masl for the bottom level and +245 masl for the upper one. Then a wireframe was interpolated following contours of matching domains between both lower and upper levels. Figure 9 shows end result of the 3D structural domain developed using assigned domains in section 4.

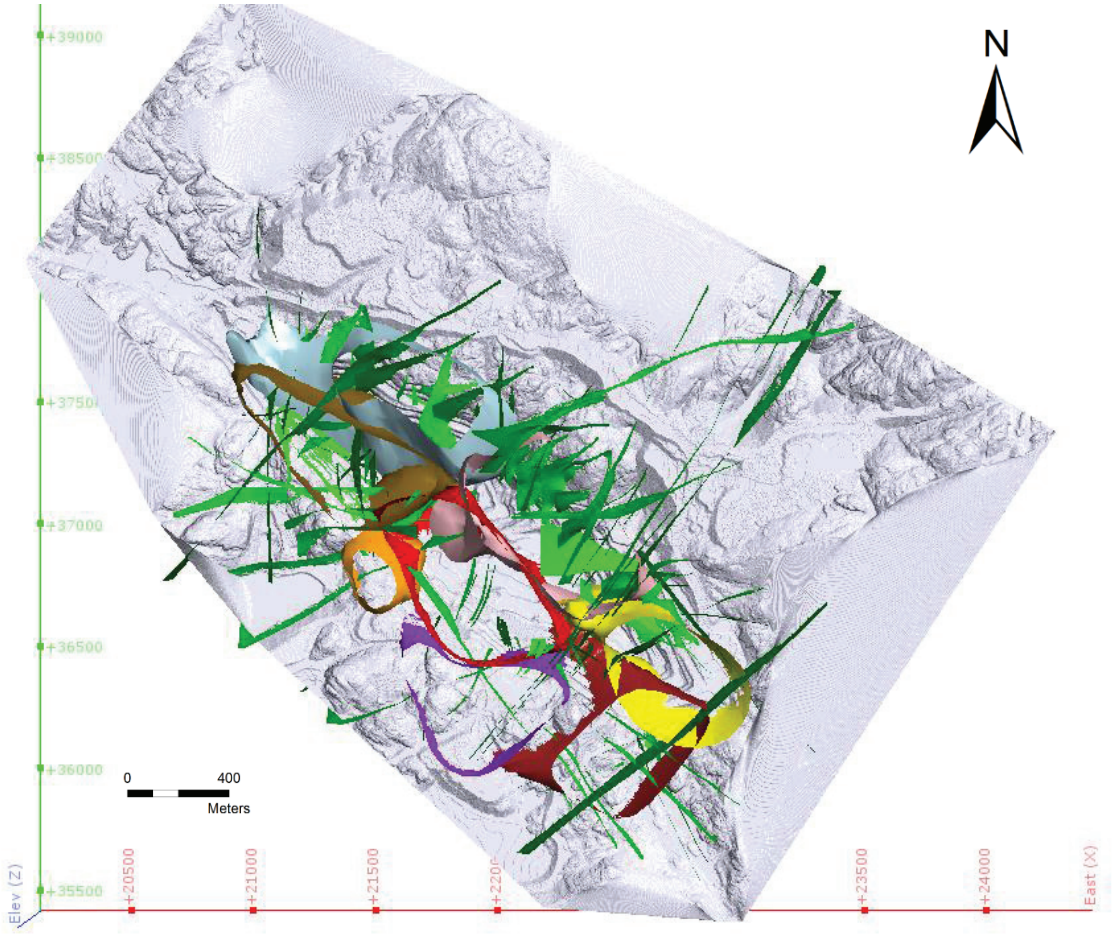

Fig. 9 **3D Structural model of the mine area, based on the connection of both the bottom and upper level and its correlation with the main discontinuities connected via field measurements. D01 (light blue); D02 (orange); D03 (pink); D04 (red); D05 (dark red); D06 (yellow); D07 (purple); D08 (brown).**

The correlation between matching domains in the two levels is also summarized in Table 3.

Table 3 **Summary of correlations between the domains in lower and upper elevation of 145 masl. Angles are in degrees.**

	Bottom (-55 to +145)				Top (+145 to +345)			
	Joint Sets (dip/dipdir)				Joint Sets (dip/dipdir)			
Domain (D)	SD	J1	J2	J3	SD	J1	J2	J3
01	145_01	90/029	89/269	-	345_07	87/215(025)	80/260	-
02	145_02	78/269	-	-	345_08	79/265	-	-
03	145_03	80/314	83/216	73/029	345_06	74/321	76/224	89/204(024)
04	145_04	54/033	61/351	81/214	345_02	43/052	56/356	76/214
05	145_05	66/223	57/056	-	345_04	85/040(220)	83/064	-
06	145_06 145_07	76/267 84/090(270)	85/235 86/056(236)	75/313 62/302	345_05	83/279	81/224	89/320
07	-	-	-	-	345_03	84/128	-	-
08	-	-	-	-	345_01	49/054	-	-

As can be seen in Table 3, there is very good correlation between upper and lower elevations of the pit. It is also clear to notice that there are joint systems that are not present in the lower portion of the pit over the depth; e.g. D07 and D08. Domains D01, D03 and D06 are mostly present in the footwall and D01, D02, D04, D05, D07 and D08 are, on the other hand, present in the hanging wall. The most dominant domain is D01, which is pronounced in both foot wall and lower levels of the hanging wall.

6 Comparative assessment

With the development of structural domain using data sets from field mapping, borehole, Sirovision and LiDAR data, it would be worthwhile to compare major findings of this study with the one carried out by Karlsen (1997), who divided mine area with six major long persisting lineaments as following (see also Figure 2):

- Hommedal (FS1) - a lineament oriented in N-S direction and very steeply dipping both towards W and E directions.
- Jossingfjord (FS2) - a lineament oriented in NE-SW or NNE-SSW direction, steeply dipping both to SE and NW with main domination to SE.
- Åna Sira (FS3) - a lineament oriented in WSW-ENE direction and dipping at 50-65 degrees in both SE and NW.
- WNW-ESE (FS4) – a lineament having dip angles between 45 and 70 degrees in SW and between 75 to 85 degrees in NE direction.
- Tellnesmyra (FS5) – a lineament oriented in NW-SE direction and dipping “gently to steep” in both NE and SW direction.
- Crusher (FS6) – a lineament having orientation close to FS5 and is dipping at angles between 45 and 65 degrees towards NE direction.

Using comprehensive data set giving detailed orientation of jointing systems of the mine, it is possible to interlink these data with these major six lineaments. Table 4 shows orientation of the major lineaments described by Karlsen (1997) and orientation of the joint systems mapped using field mapping, Sirovision, borehole and LiDAR data. As Table 4 indicates, there is a very good correlation between values presented by Karlsen (left columns) and the ones collected and analysed through this study (right columns).

Table 4 Correlation between main trends as mapped by Karlsen (1997) and as interpreted and analysed from field mapping, Sirovision, borehole and LiDAR data.

	Karlsen (1997)			This research		
	Direction	Dip Angle	DipDir	Direction	Dip/dipdir	Structural domain
FS1	N-S	90±10	W E	N-S	89/269 - 80/260 78/269 - 79/265 76/267 - 84/090	D01 D02 D06
FS2	NE-SW NNE-SSW	75±10	SE NW	NE-SW NNE-SSW	80/314 - 74/321 75/313 - 86/312 62/302 - 73/144 84/128	D03 D06 D06 D07
FS3	WSW-ENE	50-65	SSE NNW	WSW-ENE	63/345 61/351 - 56/356	D02(upper) D04
FS4	WNW-ESE	45-70 75-85	SSW NNE	WNW-ESE	87/180 76/224 - 73/029 81/214 - 76/214 85/040 - 83/064	D01 (upper) D03 D04 D05

FS5	WNW-ESE NW-SE NNW-SSE	gently to steep	NE SW	WNW-ESE NW-SE	90/029 - 87/215 83/216 - 89/204 66/223 - 57/056 85/235 - 86/056	D01 D03 D05 D06
FS6	NNW-SSE	45-65	ENE	NNW-SSE	54/033 - 43/052 49/054	D04 D08

As seen in Table 4, orientation of most of the lineaments resembles very close with the orientation of structural domains established by assessing comprehensive data from different four sources. However, there is one exception related to jointing system oriented at NNW-SSE direction of FS5 lineament. This may be explained as deficit caused by in-sufficient exposure of this joint system during field mapping conducted by Karlsen in 1997.

7 Possible failure modes

Kinematic study on the potential failure modes in the pit has also been carried out using the average dip and dip direction of jointing systems identified in each structural domain and pit slope angle. It is therefore possible that a joint set that has a dipping angle higher than the slope may lead to planar failure geometry because of the standard deviation in the dipping angle. However, it is noted here that a slope failure occurs not only based on kinematic favourability for the failure to occur, but also due to engineering geological characteristics of joint systems involved. Therefore, the results presented here should be taken as indicative potential failure modes in the defined structural domain. The slope itself has an average dip of 55 degrees (i.e. slope angle measured from corresponding bottom to the uppermost bench) and each bench face angle dips at 85 degrees (angle of the single bench). Due to unfavourable combinations of orientation of major joint systems and faults and engineering geological characteristics prevailing in the mine, several local instability events were registered in many places in north-western part of the upper pit walls. According to Nilsen and Ballou (2006), most of these incidents have occurred during heavy rainfall and during periods of repeated freezing/thawing.

In each structural domain an average slope face inclination was calculated. In most of the domains more than one typical slope was defined. In total thirteen slopes (both in hanging wall and foot wall) are identified with potential areas where slope may kinematically fail (Figure 10).

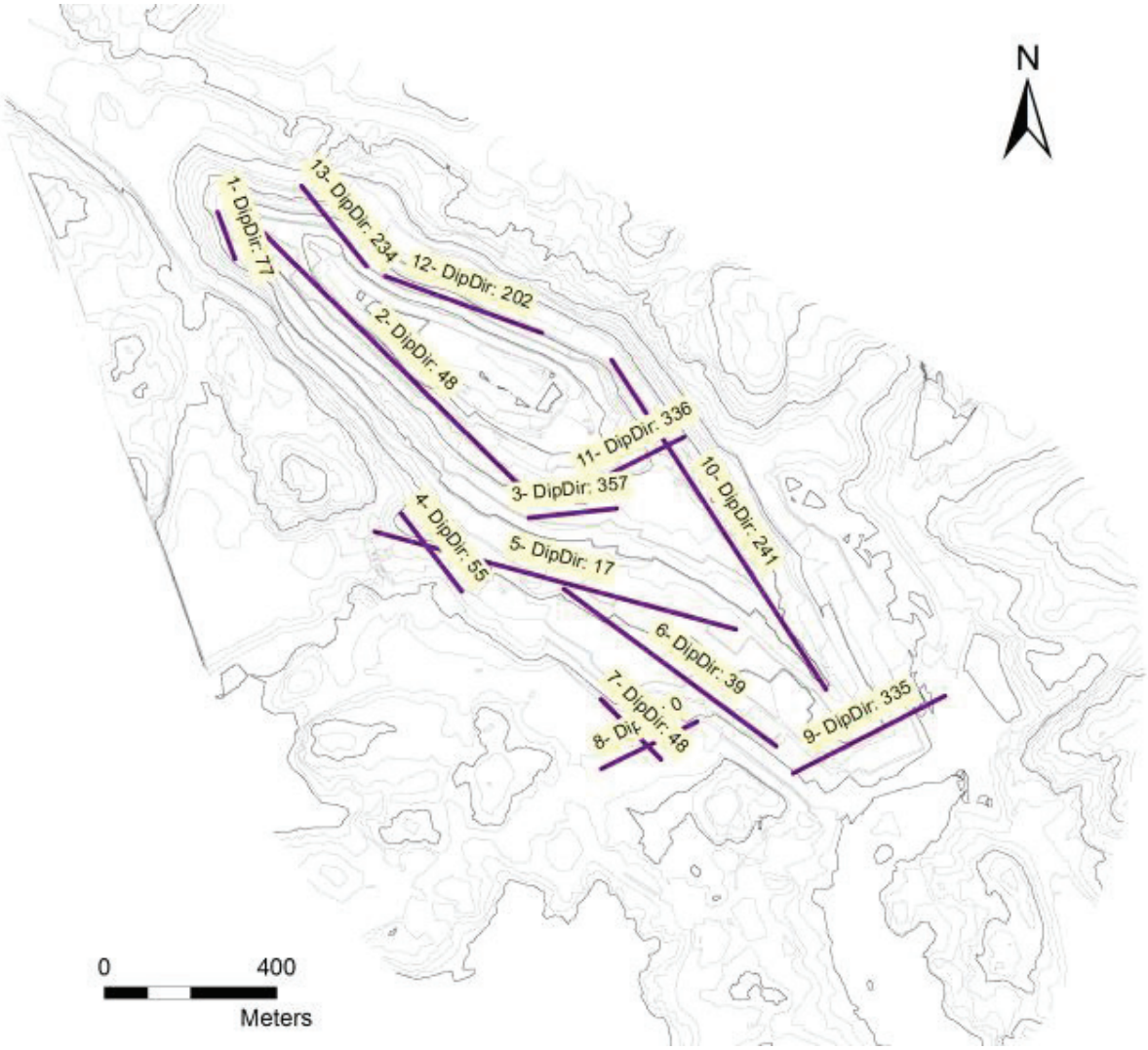

Fig. 10 Position and distribution of slopes considered for the potential failure mode analysis.

The outcome of the potential failure modes in slope scale and bench scales for hanging wall of the mine are presented in Table 5. As Table 5 indicates, kinematically there is a chance for wedge and planner failure in the overall slope of the mine in the structural domain D2, D4 and D5. On the other hand, kinematic favourability for slope failure in bench scale exist almost in all structural domain with planar, wedge and even toppling possibilities. The plane failure is mainly governed by joint set (J2) daylighting at the bench slope. This finding well coincides with the assessment presented by Nilsen and Ballou (2006), which states that there are continuous joint sets in bench scale with intermediate dip towards NE representing risk of plane failure. These surfaces contain slippery chlorite schist that make it easy for the rock mass to slide once supporting rock mass below is further excavated (Karlsen, 1997). In addition, as highlighted in Table 5, combination of joint set J1 and J2 are responsible for the formation of potential wedge failure geometry in the bench scale. These two joint sets are also causes to form blocky rock mass that are met in certain benches. This is due to their interaction with a local joint set that has a shallow dip forming tetragonal geometry and inducing individual block falls. In the same scale, it is also possible to find local toppling failure due to dip direction of joint set J3, as this joint set includes joints dipping towards SW.

Table 5 Potential failure modes in the hangingwall for each structural domain (SD). Angles are in degrees.

	Slope					Bench				
SD	Dip	DipDir	Geometry	Joint Set	Dip/Dipdir	Dip	DipDir	Geometry	Joint Set	Dip/Dipdir
D01	55	77				85	77	Planar	J2	89/88
								Toppling	J2	89/268
	55	48				85	48	Planar	J1	89/029
								Toppling	J1	89/209
D02	55	55	Wedge	J1	77/269	85	55	Wedge	J1	77/269
				J2	63/346				J2	63/346
	55	17	Wedge	J1	77/269	85	17	Planar	J2	63/346
				J2	63/346			Wedge	J1	77/269
									J2	63/346
D04	55	48	Planar	J1	43/051	85	48	Planar	J1	43/051
			Wedge	J1	43/051			Wedge	J1	43/051
				J2	56/356				J2	56/356
								Toppling	J3	75/219
	55	17	Planar	J1	43/051	85	17	Planar	J1	43/051
			Planar	J2	56/356			Planar	J2	56/356
			Wedge	J1	43/051			Wedge	J1	43/051
				J2	56/356				J2	56/356
								Toppling	J3	75/219
	55	357	Planar	J2	56/356	85	17	Planar	J2	56/356
								Wedge	J1	43/051
									J2	56/356
	55	39	Planar	J1	43/051	85	39	Planar	J1	43/051
			Wedge	J1	43/051			Wedge	J1	43/051
				J2	56/356				J2	56/356
								Toppling	J3	75/219
D05	55	39				85	39	Planar	J1	85/040
	55	335				85	335			
D07	55	48				85	48			
	55	335				85	335	Toppling	J1	84/128
D08	55	77	Planar	J1	49/054	85	77	Planar	J1	49/054
	55	48	Planar	J1	49/054	85	48	Planar	J1	49/054

Similarly, potential failure modes in slope scale and bench scales for the foot wall of the mine are presented in Table 6. As Table 6 indicates, there is less chance for total mine slope to kinematically fail. However, there is a chance for wedge, planner and toppling failure to occur at the bench scale.

In order to assess potential failure mechanism of the pit a comprehensive study of the engineering geological characteristics of each joint system is necessary and this is currently in progress under DePOPS project.

Table 6 Potential failure modes in the footwall for each structural domain (SD). Angles are in degrees.

	Slope					Bench				
SD	Dip	DipDir	Geometry	Joint Set	Dip/Dipdir	Dip	DipDir	Geometry	Joint Set	Dip/Dipdir
D01	55	202				85	202	Planar	J1	89/209
								Toppling	J1	89/029
	55	234				85	234			
D03	55	241				85	241	Planar	J3	78/218
								Wedge	J1	84/314
									J3	78/218
	55	336				85	336	Toppling	J1	84/314
								Planar	J1	84/314
								Wedge	J1	84/314
									J2	78/218
D06	55	241				85	241	Planar	J2	81/239
								Planar	J3	82/216
								Wedge	J1	78/272
									J3	82/216
	55	335				85	335	Planar	J3	79/312
								Wedge	J2	81/239
									J3	79/312
								Wedge	J1	78/272
									J2	81/239

8 Conclusions

This study clearly demonstrates that the detailed joint measurements carried out using remote sensing technique such as Sirovision and LiDAR measurements can give trustworthy results as of field mapping and may be used as part of the database for the development of 3D structural model of the mine. The deviation on data achieved from Sirovision, LiDAR and acoustic borehole in comparison to the data from field mapping were within acceptable limit. The Sirovision measurements gave an average deviation of 6.3% in dip and 4.3% in strike measurements. The LiDAR mapping has shown a deviation of 9.6% in dip and 7.6% in strike measurements and for the borehole the deviation was found to be 2.2% in dip and 15.6% in strike. Taking in account that a normal acceptable deviation in field measurements of about 5 degrees all approaches used in this study are considered to be useful.

Similarly, even though Karlsen (1997) divided the mine area with six distinct lineaments, most of the detailed jointing in this mine can be categorized in four major jointing systems defined by joint sets J1, J2, J3 and J4. However, occurrence of joint set J4 is not pronounced in the mine area due to very wide spacing. The detailed study carried out has also made it possible to divide the mine in eight major structural domains. It is also concluded that kinematically there is a chance of wedge and planar failure in the overall pit slope and wedge, planar and toppling failures in the bench slope scale of hanging wall. On the other hand, kinematically it is unlikely that the failure will occur in the overall pit slope scale in the foot wall. However, kinematically it is possible that small scale toppling, wedge and planar failure may occur in the bench scale in the foot wall too.

Therefore, a comprehensive study will be carried out to assess overall quality of the rock mass, engineering geological characteristics of all four joint sets established by this study and a comprehensive stability assessment of the pit slope in both overall slope and bench scale including susceptibility and risk assessment of this mine.

References

Botsialas, K., Mass, A. (2014) *Slope stability conditions at Tellnes Open Pit Mine. A case study and future challenges*. Mineralproduksjon vol 5 (2014) A53-A72. http://mineralproduksjon.no

Bye, A.R. (2006) *The strategic and tactical value of a 3D geotechnical model for mining optimization, Anglo Platinum, Sandsloot open pit.* The Journal of The South African Institute of Mining and Metallurgy, The South African Institute of Mining and Metallurgy, vol 106.

Bye, A.R., Bell, F.G. (2001) *Stability assessment and slope design at Sandsloot open pit, South Africa*. International Journal of Rock Mechanics & Mining Sciences, vol. 38, pp. 449–466.

Charlier, B., Skår, Ø., Korneliussen, A., Duchesne, J.C., Auwera, J.V. (2007) *Ilmenite composition in the Tellnes Fe–Ti deposit, SW Norway: fractional crystallization, postcumulus evolution and ilmenite–zircon relation.* Contributions to Mineralogy and Petrology, vol. 154, pp. 119–134

Diot, H., Bolle, O.,Lambert, J., Launeau, P., Duchesne, J. (2003) *The Tellnes ilmenite deposit (Rogaland, South Norway): magnetic and petrofabric evidence for emplacement of a Ti-enriched noritic crystal mush in a fracture zone*. Journal of Structural Geology, vol. 25, pp. 481-501.

Duchesne, J.C. (2003) *The Rogaland Intrusive Massifs - an excursion guide*. Norges geologiske undersøkelse, Trondheim. Report no.: 2001.029.

Gigli G, Casagli N. (2011) Semi-automatic extraction of rock mass structural data from high resolution LIDAR point clouds. International Journal of Rock Mechanics and Mining Sciences. 48 (2): 187-198.

Gigli G, Frodella W, Garfagnoli F, Morelli S, Mugnai F, Menna F, Casagli N. (2014) 3-D geomechanical rock mass characterization for the evaluation of rockslide susceptibility scenarios. Landslides, DOI 10.1007/s10346-013-0424-2.

Gigli, G., Farina, P. (2016) *LiDAR scanning of Tellnes Open Pit.* Internal report. 102p

Haines, A., Terbrugge, P.J., Carrieri, G. (1991) *Preliminary Estimation of Rock Slope Stability Using Rock Mass Classification Systems*. International Society for Rock Mechanics, published in the 7th ISRM Congress.

Hanson, C. Thomas, D. and Gallagher, B. (2005) *The Value of Early Geotechnical Assessment in Mine Planning*, in Aziz, N (ed), Coal 2005: Coal Operators' Conference, University of Wollongong and the Australasian Institute of Mining and Metallurgy, pp. 17-30.

Hormazabal, E., Rovira, F., Walker, M., Carranza-Torres, C. (2009) *Analysis and design of slopes for Rajo Sur, an open pit mine next to the subsidence crater of El Teniente mine in Chile.* Slope Stability, Santiago Chile, November 2009.

Karlsen, T. A. (1997) *Geometry of fracture zones and their influence on the quality at the Tellnes mine, Rogaland*. Norges geologiske undersøkelse, Trondheim. Report no.:97.031.

Langåker, M.Ø., Gylland, A.S., Jacobsen, K.W., Yri, T. (2015) *Tellnes Gruve – Tunnelinspeksjon/Ingeniørgeologisk Kartlegging Av Tunneler.* Sweco Norge AS. Internal Report 13711001-R01-A01. 94p.

Marker, M., Schiellerup, H., Meyer, G.B., Robins, B. & Bolle, O. (2003) *The Rogaland Anorthosite Province*. Geological map 1:75000. Norges geologiske undersøkelse, Trondheim. Special Publication 9, 109-116.

Nilsen, B., Ballou, B.J. (2006) *Stability Problems and Rock Support at the Tellnes Open Pit Mine, Norway.* The South African Institute of Mining and Metallurgy International Symposium of Stability of Rock Slopes: 155-165.

Palmstrom, A. (2005) *Measurements of and Correlations between Block Size and Rock Quality Designation (RQD).* Tunnels and Underground Space Technology, vol. 20, pp. 362-377.

Pantelidis, L. (2009) *Rock slope stability assessment through rock mass classification systems*. International Journal of Rock Mechanics & Mining Sciences, vol. 46, pp. 315–325.

Park, H.J., West, T.R. (2002). *Sampling bias of discontinuity orientation caused by linear sampling technique*. Engineering Geology, vol 66. pp 99-100

Priest, S.D. and Hudson, J.A. (1981) *Estimation of discontinuity spacing and trace length using scanline surveys.* International Journal of Rock Mechanics and Mining Science & Geomechanics, vol. 18, no. 3, pp. 183-197.

Riglar, B., Varga, V. (2014) *Final Report on borehole geophysical logging and hydraulic testing in 11 boreholes for Titania AS.* Ruden AS. Internal Report. Project numner P109-2014. 275pp.

Riquelme, A.J., Abellán, A., Tomás, R. (2015). Discontinuity spacing analysis in rock masses using 3D point clouds. Engineering Geology 195, pp. 185-195.

Riquelme, A.J., Tomás, R., Abellán, A. (2016). Characterization of rock slopes through slope mass rating using 3D point clouds. Int J Rock Mech Mining Sci http://dx.doi.org/10.1016/j.ijrmms.2015.12.008i

Villaescusa, E. and Brown, E.T. (1992) *Maximum Likelihood Estimation of Joint Size from Trace Length Measurements*. Rock Mech. & Rock Eng, vol. 25, pp 67-87.

Willie, D.C., Mah, C.W. (2004). *Rock Slope Engineering. Civil and Mining.* 4th edition, pp. 41-42.

Yamane, Taro. (1967). Statistics: An Introductory Analysis, 2nd Ed., New York: Harper and Row.

Yuri Lee , Dong-Woo Ryu & Hi-Keun Lee (2000) *An Application of Stereophotogrammetry in Investigating Rock Discontinuity Orientation*, Geosystem Engineering, 3:2, 71-80, DOI: 10.1080/12269328.2000.10541154

Zhang, L.., Einstein, H.H. (2004) *Using RQD to estimate the deformation modulus of rock masses*. International Journal of Rock Mechanics & Mining Sciences, vol. 41, pp. 337–341.